ACS APPLIED OPTICAL MATERIALS

pubs.acs.org/acsaom

Article

Dicyclohexyl(phenyl)phosphine Oxide-Based Neutral Manganese(II) Bromide Scintillator for X-ray Imaging

Published as part of ACS Applied Optical Materials special issue "Phosphor Safari 2024".

Xiaokang Zheng, Peng Tao,* Hua Wang,* and Wai-Yeung Wong*

Cite This: ACS Appl. Opt. Mater. 2025, 3, 942−948

Read Online

ACCESS | Metrics & More | Article Recommendations | Supporting Information

ABSTRACT: Luminescent manganese(II) halide-based materials have drawn increasing research interest because of their rich photophysical properties. The good understanding of the relationships between the photophysical property and the molecular structure of the manganese(II) complex could give deep insights to further guide the structural design of the manganese(II) emitters. Currently, neutral manganese(II) halides based on the monodentate ligand mainly rely on triarylphosphine oxide. To extend this family of luminescent manganese(II) halides, herein, by introducing two bulky cyclohexyl moieties bonded to the phosphorus atom, we employ a dicyclohexyl(phenyl)phosphine oxide (DCPPO) to synthesize manganese(II) bromide (**DCPPOMnBr**). The prepared manganese(II) complex not only exhibits green room-temperature photoluminescence peaking at 508 nm with narrowband emission and a photoluminescence lifetime of 0.112 ms but also shows zero-thermal-quenching luminescence below 260 K in the solid state under ultraviolet light. The complex further serves as the scintillator for high spatial resolution X-ray imaging (10.52 lp mm^{-1}). These results clearly demonstrate that the proposed ligand design strategy can be an effective way to extend such a family of manganese(II) emitters and will provide further insights into their relationships between the molecular structure and photophysical properties.

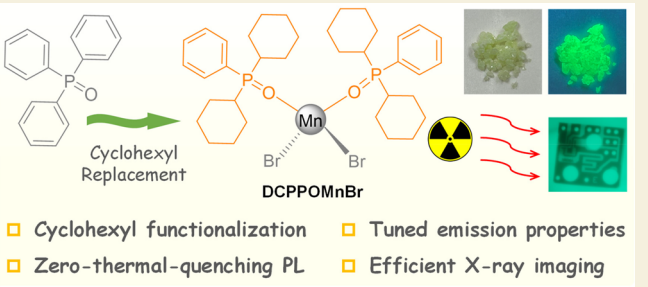

KEYWORDS: *luminescence, manganese(II) halide, scintillator, structure-property relationship, X-ray imaging*

INTRODUCTION

Transition-metal-based luminescent materials have been proved to be an important class of photofunctional semiconductors, which have been widely involved in organic electronic devices, photocatalysis, biomedical engineering, etc.[1−6] Compared with the noble metal-based light-emitting complexes, the cheap metal-based ones attracted an increasing interest because of their rich abundance and low cost.[7−10] Recently, the manganese(II) halide-based luminescent emitters become an emerging generation of photofunctional materials attributed to their intriguing photophysical properties (e.g., intense luminescence in the solid state, adjustable emission energy and lifetimes, etc).[11−14] The radiative deactivation from the $^4T_1$ excited state to the $^6A_1$ ground state in the manganese(II) centers is responsible for the light emission of the manganese(II) halides.[15−17] The coordination number of the manganese(II) center and the nature of ligands will determine the emission energy by altering the crystal field strength, thereby resulting in a wide tunability of the emission color ranging from the green to the near-infrared.[18−20]

As a typical type of manganese(II)-based emitters, the neutral luminescent manganese(II) halides are usually made up of the phosphine oxide ligands and halide ligands (e.g., Cl^-, Br^-, or I^-).[21−23] Besides the halide ligands, the molecular design of the phosphine oxide ligands has become the research focus to manipulate the photophysics of such manganese(II) complexes.[24] The reported organic phosphine oxide ligands for developing manganese(II) halide-based emitters mainly include monodentate and bidentate ones. The manganese(II) emitters supported by the bidentate ligands normally show higher photoluminescence (PL) quantum yields (PLQYs) than that of the monodentate ligand-based ones at room temperature.[25] For instance, the bis(2-(diphenylphosphino)phenyl)-ether oxide was used by Guo and co-workers to construct the tetrahedral manganese(II) complexes showing bright green room-temperature luminescence with PLQY as high as 70% in the solid states owing to the rigidity of the bridging oxygen in the phosphine oxide ligand.[26] However, the tetrahedral manganese(II) complexes based on the monodentate

Received: January 30, 2025
Revised: March 20, 2025
Accepted: March 21, 2025
Published: April 2, 2025

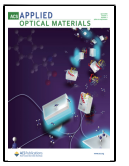

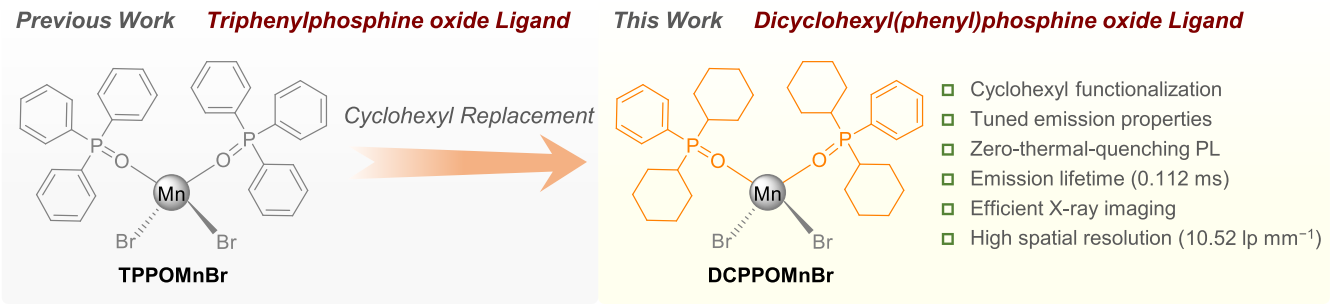

Figure 1. Rational design of dicyclohexyl(phenyl)phosphine oxide-based neutral manganese(II) bromide scintillator (**DCPPOMnBr**) for X-ray imaging.

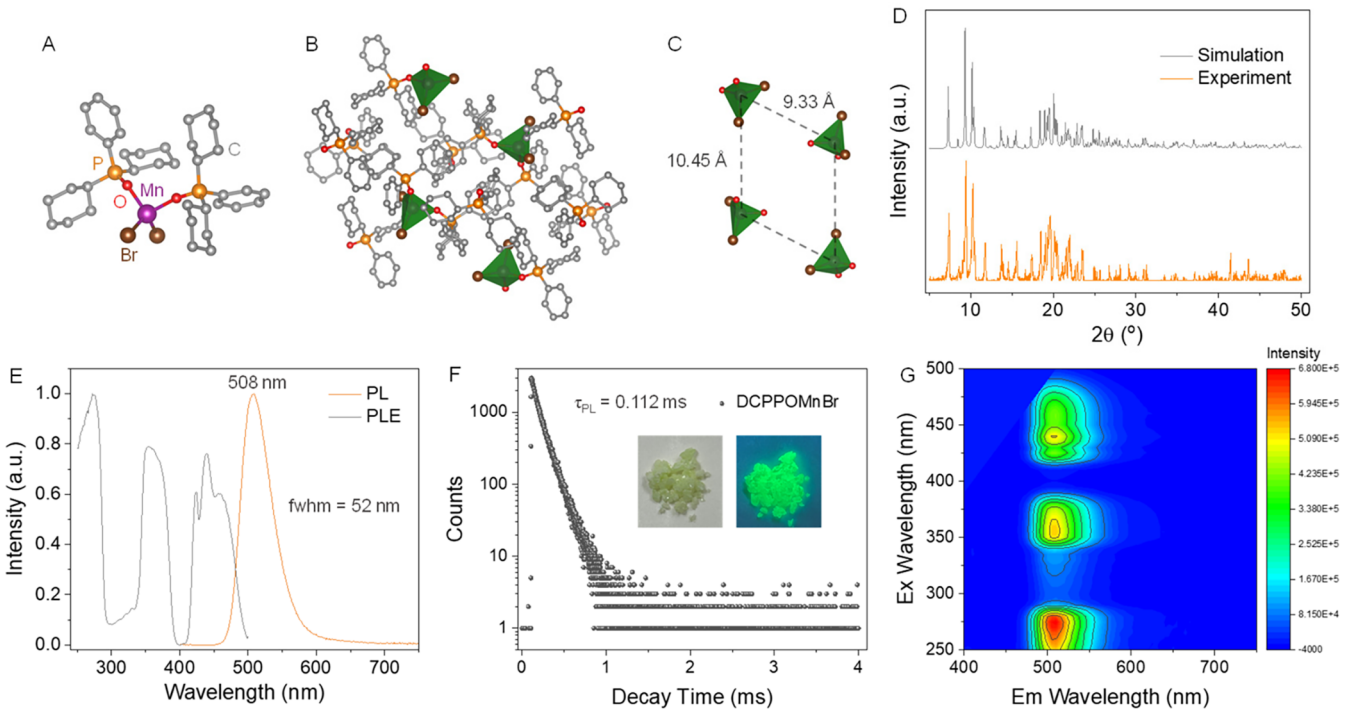

Figure 2. Crystal structure (A), molecular packing (B), and Mn−Mn distances (C) of **DCPPOMnBr** (CCDC 2418713, the hydrogen atoms omitted for clarity) at room temperature. Measured and simulated powder X-ray diffraction (PXRD) (D) of **DCPPOMnBr**. The PLE spectrum monitored at 508 nm and PL spectrum excited at 275 nm (E), time-resolved PL decay curve (λ_{ex} = 275 nm) (F), and excitation-emission PL spectrum (G) of **DCPPOMnBr** in the crystal state at room temperature. Insets show the photographs of the **DCPPOMnBr** crystal under room light (left) and UV light of 365 nm (right).

triphenylphosphine oxide in the solid states are either weakly emissive or nonemissive at room temperature.[26,27] Later, a family of the monodentate phosphoramide-based manganese(II) complexes designed by Jin et al. also exhibit poor PLQYs.[26,28] To date, the performances of the monodentate ligand-based manganese(II) emitters are far behind those of the bidentate ligand-based ones, thus hindering their further applications in photoelectronics.[25,29] Therefore, it is essential to extend this family of luminescent Mn(II) halides, and there are many opportunities to develop neutral monodentate ligand-based manganese(II) halides through the rational design of ligands. The reported manganese(II) emitters with monodentate ligands are mainly based on the triphenylphosphine oxides and their derivatives.[25,29−32] The alkyl moieties are rarely involved in the monodentate ligand design for manganese(II) emitters, particularly for the alkyl groups directly bonded to the phosphorus atom.[25,29−32] The cyclohexyl moiety as the typical alkyl group can provide an effective steric hindrance effect to maintain an appropriate Mn−Mn distance and reduce manganese(II) concentration quenching, suggesting that it would be a useful building block for such ligand design.

In this work, we developed a new neutral manganese(II) bromide (**DCPPOMnBr**) with monodentate ligands by incorporating two bulky cyclohexyl moieties bonded to the phosphorus atom to construct a cyclohexyl-based monodentate ligand [i.e., dicyclohexyl(phenyl)phosphine oxide (DCPPO)] (Figure 1). The manganese(II) complex supported by the DCPPO ligand not only showed green room-temperature light emission peaking at 508 nm with a narrow full width at half maxima (fwhm) of 52 nm and emission lifetime (τ_{PL}) of 0.112 ms but also possessed zero-thermal-quenching (ZTQ) luminescence below 260 K in the solid state under ultraviolet light. The complex was further employed as the scintillator for X-ray imaging with a high spatial resolution of 10.52 lp mm^{-1} and a relatively low detection limit of 0.1057 μGy$_{air}$ s^{-1}. The

https://doi.org/10.1021/acsaom.5c00040
ACS Appl. Opt. Mater. 2025, 3, 942−948

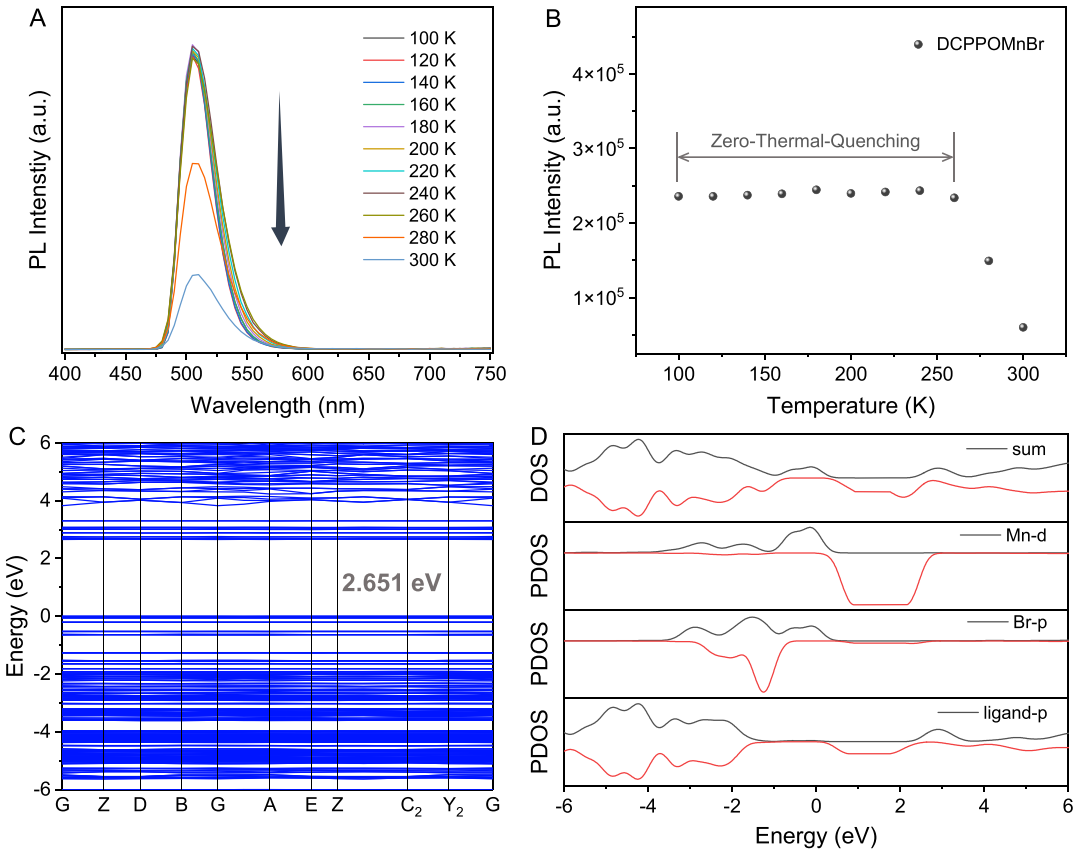

Figure 3. PL spectra (A) and PL intensity variations (B) of **DCPPOMnBr** in the crystal state at different temperatures (λ_{ex} = 275 nm). Simulated energy-band structure (C) and density of states (DOS) (D) of **DCPPOMnBr** in the crystal state.

ligand design strategy in this work will give new insights into the relationships between the molecular structure and photophysical properties of the neutral manganese(II) emitters.

RESULTS AND DISCUSSION

Synthesis and Characterization

The dicyclohexyl(phenyl)phosphine oxide ligand was obtained from a commercial source. As shown in Scheme S1, under an air atmosphere, the ligand can easily coordinate with $MnBr_2 \cdot 4H_2O$ in the mixed solutions of dichloromethane and ethanol at 25 °C. A pale green powder was obtained after the removal of the solvents under vacuum. The yellowish green block crystals of the target complex were further cultivated in a high yield of 70% from the mixed solvents of *n*-hexane and dichloromethane by slowly evaporating solvents at room temperature. The structure of **DCPPOMnBr** in the solid state was confirmed by single-crystal X-ray diffraction. As shown in Figure 2A,B, the crystals crystallized in the monoclinic $P2_1/c$ space group with no solvent molecule embedded in the crystal (Table S1), and the manganese(II) center adopted a slightly distorted tetrahedral configuration with the bond angles of 119.09° for Br−Mn−Br and 100.87° for O−Mn−O (Table S2). The bond lengths of two Mn−Br bonds are 2.47 and 2.48 Å, while the bond lengths (2.02 and 2.03 Å) of two Mn−O bonds are shorter than those for the Mn−Br bonds. The observed bond parameters for **DCPPOMnBr** are well consistent with the reported analogues.[5,7]

The exclusion of the solvent molecules in the crystal lattice implied that the neutral molecules of **DCPPOMnBr** can pack together tightly to generate very stable crystals through the weak van der Waals intermolecular interactions. For example, the distances of the short contacts between the Br and H atoms in cyclohexyl moieties are 2.81 and 3.01 Å, respectively, and the distances of the C−H···π interactions are 2.81 to 3.35 Å, respectively (Figure S1). The distances between the adjacent manganese(II) center in the crystal are 9.33 and 10.45 Å, respectively (Figure 2C), which is longer than that of the reported analogue,[7] which could be attributed to the relatively bulky cyclohexyl moieties. The enhanced distance between the adjacent manganese(II) center could further inhibit the energy migration between metal centers in the excited states to minimize the PL quenching in the crystal state. Moreover, the good agreement of the simulated PXRD pattern with the experimental one suggested the phase purity of the prepared crystals (Figure 2D). The temperature-dependent PXRD patterns exhibited negligible changes within the range 100−300 K, indicating the absence of the phase transition (Figure S2A). As presented in Figure S2B, the differential scanning calorimetry curve exhibited a sharp endothermic peak located at 246.5 °C during heating, which corresponds to the melting point of the crystals.

The thermal stability of **DCPPOMnBr** in the crystal state was evaluated by using thermogravimetric analysis under a N_2 atmosphere. It was observed that the temperature of weight loss at 5% of the crystals was as high as 394 °C (Figure S3), indicating that the very high thermal stability of the crystals was attributed to the close packing of the complex molecules.

https://doi.org/10.1021/acsaom.5c00040
ACS Appl. Opt. Mater. 2025, 3, 942−948

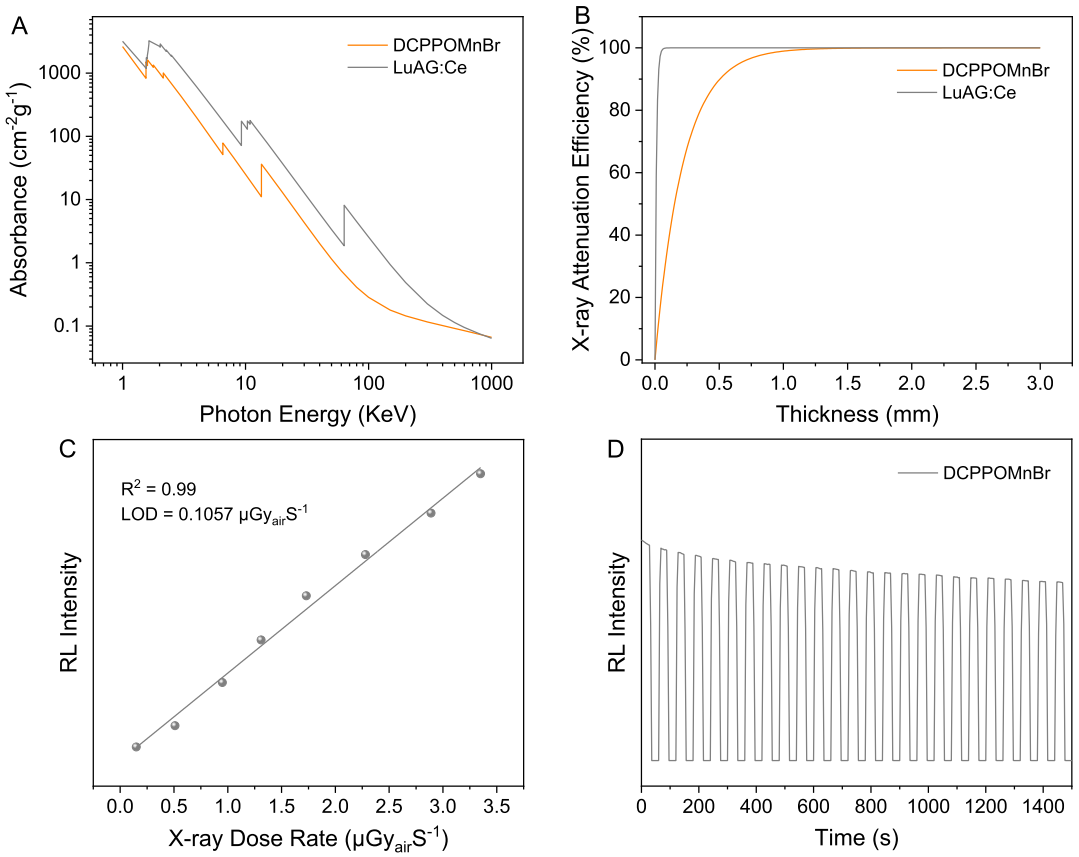

Figure 4. X-ray absorbance of high-energy photons of **DCPPOMnBr** and LuAG:Ce (A). X-ray attenuation efficiencies of **DCPPOMnBr** and LuAG:Ce with different thicknesses (B). Linear dependence between the RL intensity of the **DCPPOMnBr** crystal and X-ray dose rate with the LOD confirmed at a SNR of 3 (C). X-ray irradiation stability of the **DCPPOMnBr** crystal upon X-ray irradiation for 25 cycles. X-ray irradiation was switched on for 30 s and then switched off for 30 s in each cycle (D).

Photophysical Properties under UV Light

As shown in Figure 2E, the complex crystals exhibits a green room-temperature luminescence (508 nm) with a narrow fwhm of 52 nm under the UV light of 275 nm, which is originated from the typical $^4T_1(G) \rightarrow {}^6A_1$ radiative electronic transition in manganese(II) center.[25] Due to the enhanced spin-orbit coupling induced by the heavy-atom effect of the bromine atom, the complex shows a PL lifetime of 0.112 ms (Figure 2F and Table S3), which is similar to the reported manganese(II) bromides.[30] The 1931 Commission Internationale de l'Elcairage (CIE) coordinates for the PL spectrum was determined to be (0.18, 0.62). The complex **DCPPOMnBr** shows a moderate PLQY of 9.72% in the crystal state at room temperature (Table S3), which is comparable to that of the reported monodentate ligand-based neutral manganese(II) halides.[25,30] A multiple band is observed for the photoluminescence excitation (PLE) spectrum monitored at 508 nm for the complex (Figure 2E), the three excitation bands from the high energy band to the low energy band should have originated from the electronic transitions of $^6A_1 \rightarrow {}^4T_1(F)/{}^4A_2(F)$, $^6A_1 \rightarrow {}^4E(D)/{}^4T_1(P)$, and $^6A_1 \rightarrow {}^4T_1(G)/{}^4T_2(G)/{}^4A_1(G)/{}^4E(G)$ in the tetrahedral manganese(II) center.[7] The excitation-emission mapping showed no emission peak shift when the excitation wavelength was changed (Figure 2G), indicating that the green emission originated from the same excited state without other impurities. It should be noted that the PLQY for **DCPPOMnBr** is much lower than that of the bidentate ligand-based complexes,[25,31] which may be caused by the flexibility of the monodentate dicyclohexyl(phenyl)phosphine oxide ligand, leading to an accelerated nonradiative deactivation process with a large nonradiative decay rate (k_{nr}) of 8.061 ms^{-1} that is much higher than the radiative decay rate (k_r) of 0.868 ms^{-1}. The temperature-dependent PL was further explored for the complex. From Figure 3AB, the PL intensity remarkably decreased from the temperature of 260 to 300 K. However, when the temperature decreased from 260 to 100 K, the PL intensity remained unchanged, implying that the complex possesses an excellent zero-thermal-quenching luminescent property below 260 K.[32]

To gain a deeper understanding of the electronic structure of the **DCPPOMnBr** crystals, we further calculated the electronic structure of this complex through the density functional theory. As depicted in Figure 3C, the simulated band structure of **DCPPOMnBr** crystal shows the flat band edges of valence band maximum (VBM) and conduction band minimum (CBM), implying the negligible wave function overlap and weak coupling effect between Mn tetrahedron. The estimated band gap value of this complex was 2.651 eV. According to the simulated DOS in Figure 3D, the VBM mainly consists of Br 2p and Mn 3d atomic orbitals, while the CBM is mainly composed of the 2p atomic orbitals of the ligands. Furthermore, from Figure S4, the charge density distributions of VBM mainly distribute over the tetrahedral center of **DCPPOMnBr**, and the charge density distributions of CBM are localized in the phenyl moieties of the ligands, suggesting

https://doi.org/10.1021/acsaom.5c00040
ACS Appl. Opt. Mater. 2025, 3, 942−948

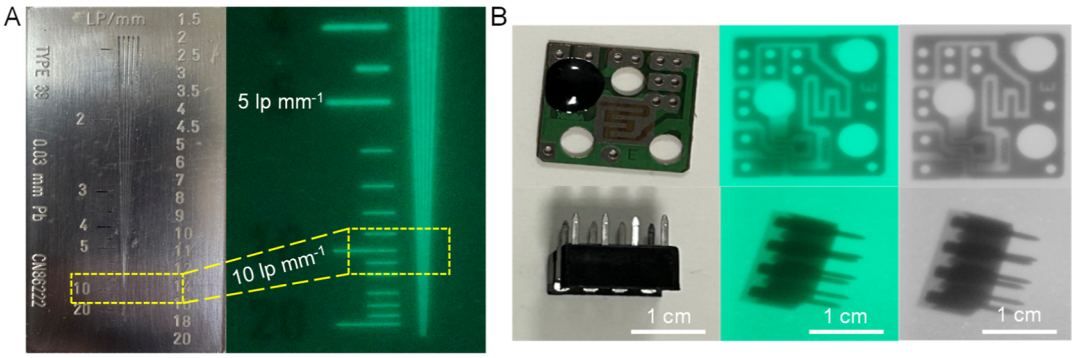

Figure 5. Photograph and X-ray image of a standard X-ray line-pair resolution phantom (A). X-ray images of a chip (up) and IC Socket (down) (B) based on the **DCPPOMnBr**-based film scintillator.

both the manganese(II) center and ligands are involved in the luminescence of the complex.

Radioluminescence under X-ray

We further investigated the radioluminescence (RL) properties of **DCPPOMnBr** crystals. The calculated X-ray absorbance of **DCPPOMnBr** was slightly lower than the commercial scintillator $Lu_3Al_5O_{12}$/Ce (LuAG/Ce) due to the lower effective atomic numbers (Z_{eff}) (Figure 4A). The X-ray attenuation efficiency of **DCPPOMnBr** with different thicknesses were also calculated, which exhibited 80% of X-ray attenuation efficiency at a thickness of 0.5 mm (Figure 4B). Under the excitation of the X-ray radiation, the **DCPPOMnBr** crystals display an intense green radioluminescence, which is the same as the PL spectrum under the UV light (Figure S5). The intensity of the radioluminescence enhances linearly with the increase in the X-ray dose rate (Figures 4C and S4). As shown in Figure 4C, the limit of detection (LOD) was determined to be 0.1057 μGy_{air} s^{-1} for **DCPPOMnBr** (signal-to-noise ratio at 3), suggesting the LOD of this complex is lower than that of the medical diagnosis criteria (5.5 μGy s^{-1}). The relative light yield of **DCPPOMnBr** is 2193 photons MeV^{-1} by using LuAG:Ce (25,000 photons MeV^{-1}) as the reference (Figure S6). The relatively low light yield should arise from the low PLQY of the complex. The stability of **DCPPOMnBr** to X-ray irradiation was also evaluated by monitoring the RL intensity change upon X-ray irradiation for 25 cycles (Figure 4d). The RL intensity of **DCPPOMnBr** decreased by 18.7% after 25 cycles of on-off X-ray irradiation, implying relatively high irradiation stability for **DCPPOMnBr**.

X-ray Imaging Performance

We further attempted to use complex **DCPPOMnBr** as the dopant emitter to prepare the scintillation screen. A scintillation screen with an edge length of 2.5 cm was then prepared by doping the complex into the poly(methyl methacrylate) (PMMA) host through a drop-casting method. The obtained film scintillator exhibited uniform green luminescence under UV light (Figure S7), implying that the fine crystals of the complex were dispersed uniformly in the PMMA host. X-ray imaging was carried out by a self-built X-ray imaging system (Figure S8). As depicted in Figure 5A, the prepared scintillation screen realized a high spatial resolution of ~10 lp mm^{-1}, which is almost comparable to that of the scintillation screens composed of the neutral manganese(II) complexes with high PLQYs.[33] We also calculated the modulation transfer function using the slanted-edge method (Figure S9). The calculated spatial resolution is 10.52 lp mm^{-1}, demonstrating excellent consistency with the line-pair resolution phantom imaging result. This result indicates that there is no inherent correlation between the spatial resolution of X-ray imaging and the PLQY of the doped emitters.[34] Subsequently, as shown in Figure 5B, the X-ray imaging performance of the scintillation screen was evaluated by using the planar chip and three-dimensional IC Socket at a dose rate of 147.6 μGy s^{-1}. Because of the difference in X-ray absorbance between the plastics and the metals, the circuit structure and internal configuration of these objects were clearly displayed in the X-ray images, suggesting that the scintillation screen prepared from the new complex shows great potential in X-ray imaging.[35−37] To better understand the X-ray imaging properties of **DCPPOMnBr**, the commercial scintillator CsI:Tl was selected as a reference to compare the image clarity between the **DCPPOMnBr** scintillation screen and CsI:Tl within the dose rates from 23.12 μGy s^{-1} to 147.6 μGy s^{-1}. Specifically, a metallic spring in the capsule and a chip were utilized as the imaging objects (Figure S10). The results showed that the **DCPPOMnBr** scintillation screen exhibits an excellent X-ray imaging performance.

CONCLUSIONS

In summary, we have proposed a cyclohexyl functionalization strategy for the development of a monodentate ligand-based neutral manganese(II) halide. A new manganese(II) complex **DCPPOMnBr** was prepared via the incorporation of two bulky cyclohexyl moieties into their phosphine oxide ligands, where the cyclohexyl unit was directly bonded to the phosphorus atom. Under the excitation of UV light, the as-prepared manganese(II) complex showed bright green luminescence (508 nm) with a moderate PLQY of 9.72% and a narrow fwhm of 52 nm as well as an emission lifetime of 0.112 ms in the crystal state at room temperature. More notably, this complex also exhibited zero-thermal-quenching luminescence in the solid state under UV light below 260 K. In addition, the complex was further used as the dopant to prepare the scintillation screen for X-ray imaging with a high spatial resolution of 10.52 lp mm^{-1} and a relatively low detection limit of 0.1057 μGy_{air} s^{-1}. Our work indicated that the bulky cyclohexyl group would be a useful building block for the further exploration of the monodentate ligand-based neutral manganese(II) halide molecules and will contribute to the better understanding of their structure-property relationships.

https://doi.org/10.1021/acsaom.5c00040
ACS Appl. Opt. Mater. 2025, 3, 942−948

EXPERIMENTAL SECTION

The detailed information (e.g., starting materials, reagents, methods, characterization, scintillation film fabrication, etc.) can be found in the Supporting Information.

Synthesis of Complex DCPPOMnBr

Dicyclohexyl(phenyl)phosphine oxide (DCPPO) (10 mmol) in dichloromethane (10 mL) was added to a solution of ethanol (5 mL) containing $MnBr_2 \cdot 4H_2O$ (5 mmol) under an air atmosphere, and the mixture was stirred for 12 h at 25 °C. The solvent was removed under vacuum, and a pale green powder was obtained, which was further used to cultivate the single crystals (yellowish green crystals with a yield of 70%) from the mixed solvents of dichloromethane and *n*-hexane by slowly evaporating solvents at 25 °C.

ASSOCIATED CONTENT

Supporting Information

The Supporting Information is available free of charge at https://pubs.acs.org/doi/10.1021/acsaom.5c00040.

Materials and methods; X-ray structure determination; computational methods; fabrication of scintillation film; X-ray light yield measurements; synthetic route, crystallographic data, selected bond lengths and angles, photophysical properties, weak interactions in **DCPPOMnBr** crystals, PXRD, TGA, calculated VBM and CBM, RL spectra, self-built X-ray imaging system, and MTF curve (PDF)

Supplementary crystallographic data for complex **DCPPOMnBr** (CIF)

Accession Codes

Accession Codes CCDC 2418713 contains the supplementary crystallographic data for this paper. These data can be obtained free of charge via www.ccdc.cam.ac.uk/data_request/cif, or by emailing data_request@ccdc.cam.ac.uk, or by contacting The Cambridge Crystallographic Data Centre, 12 Union Road, Cambridge CB2 1EZ, UK; fax: +44 1223 336033.

AUTHOR INFORMATION

Corresponding Authors

Peng Tao − *Department of Applied Biology and Chemical Technology and Research Institute for Smart Energy, The Hong Kong Polytechnic University, Hong Kong 999077, P. R. China; The Hong Kong Polytechnic University Shenzhen Research Institute, Shenzhen 518057, P. R. China;* orcid.org/0000-0003-1932-557X; Email: pengtao@polyu.edu.hk

Hua Wang − *MOE Key Laboratory of Interface Science and Engineering in Advanced Materials, Taiyuan University of Technology, Taiyuan 030024, P. R. China; College of Textile Engineering, Taiyuan University of Technology, Jinzhong 030600, P. R. China;* orcid.org/0000-0002-2976-9521; Email: wanghua001@tyut.edu.cn

Wai-Yeung Wong − *Department of Applied Biology and Chemical Technology and Research Institute for Smart Energy, The Hong Kong Polytechnic University, Hong Kong 999077, P. R. China; The Hong Kong Polytechnic University Shenzhen Research Institute, Shenzhen 518057, P. R. China;* orcid.org/0000-0002-9949-7525; Email: wai-yeung.wong@polyu.edu.hk

Author

Xiaokang Zheng − *MOE Key Laboratory of Interface Science and Engineering in Advanced Materials, Taiyuan University of Technology, Taiyuan 030024, P. R. China; Department of Applied Biology and Chemical Technology and Research Institute for Smart Energy, The Hong Kong Polytechnic University, Hong Kong 999077, P. R. China; The Hong Kong Polytechnic University Shenzhen Research Institute, Shenzhen 518057, P. R. China;* orcid.org/0000-0003-0410-1063

Complete contact information is available at: https://pubs.acs.org/10.1021/acsaom.5c00040

Notes

The authors declare no competing financial interest.

ACKNOWLEDGMENTS

We acknowledge the financial support from the National Natural Science Foundation of China (61905120, 52073242, and 62074109), Start-up Fund for RAPs under the Strategic Hiring Scheme (P0035922), the Hong Kong Research Grants Council (PolyU 15305320), CAS-Croucher Funding Scheme for Joint Laboratories (ZH4A), and Miss Clarea Au for the Endowed Professorship in Energy (847S).

REFERENCES

(1) Zhang, K. Y.; Yu, Q.; Wei, H.; Liu, S.; Zhao, Q.; Huang, W. Long-Lived Emissive Probes for Time-Resolved Photoluminescence Bioimaging and Biosensing. *Chem. Rev.* **2018**, *118*, 1770−1839.

(2) Yam, V. W.-W.; Au, V. K.-M.; Leung, S. Y.-L. Light-Emitting Self-Assembled Materials Based on d^8 and d^{10} Transition Metal Complexes. *Chem. Rev.* **2015**, *115*, 7589−7728.

(3) Tao, P.; Lü, X.; Zhou, G.; Wong, W.-Y. Asymmetric *Tris*-Heteroleptic Cyclometalated Phosphorescent Iridium(III) Complexes: An Emerging Class of Metallophosphors. *Acc. Mater. Res.* **2022**, *3*, 830−842.

(4) Huang, C.; Liang, C.; Sadhukhan, T.; Banerjee, S.; Fan, Z.; Li, T.; Zhu, Z.; Zhang, P.; Raghavachari, K.; Huang, H. In-vitro and In-vivo Photocatalytic Cancer Therapy with Biocompatible Iridium(III) Photocatalysts. *Angew. Chem., Int. Ed.* **2021**, *60*, 9474−9479.

(5) Qin, Y.; Tao, P.; Gao, L.; She, P.; Liu, S.; Li, X.; Li, F.; Wang, H.; Zhao, Q.; Miao, Y.; Huang, W. Designing Highly Efficient Phosphorescent Neutral Tetrahedral Manganese(II) Complexes for Organic Light-Emitting Diodes. *Adv. Optical Mater.* **2019**, *7*, 1801160.

(6) Tan, G.-H.; Chen, Y.-N.; Chuang, Y.-T.; Lin, H.-C.; Hsieh, C. A.; Chen, Y.-S.; Lee, T.-Y.; Miao, W.-C.; Kuo, H.-C.; Chen, L.-Y.; Wong, K.-T.; Lin, H.-W. Highly Luminescent Earth-Benign Organometallic Manganese Halide Crystals with Ultrahigh Thermal Stability of Emission from 4 to 623 K. *Small* **2022**, *19*, 2205981.

(7) Zheng, X.; Zhou, Z.; Li, Z.; Tran, K.-T.; She, P.; Wang, H.; Wong, W.-Y.; Zhao, Q.; Tao, P. Designing an Aromatic Moiety-Free Neutral Luminescent Manganese(II) Halide Scintillator for Efficient X-ray Imaging. *J. Mater. Chem. C* **2024**, *12*, 8296.

(8) Wei, Y.-L.; Jing, J.; Shi, C.; Ye, H.; Wang, Z.; Zhang, Y. High Quantum Yield and Unusual Photoluminescence Behaviour in Tetrahedral Manganese(II) Based on Hybrid Compounds. *Inorg. Chem. Front.* **2018**, *5*, 2615−2619.

(9) Zhou, G.; Ren, Q.; Molokeev, M. S.; Zhou, Y.; Zhang, J.; Zhang, X.-M. Unraveling the Ultrafast Self-assembly and Photoluminescence in Zero-Dimensional Mn^{2+}-Based Halides with Narrow-Band Green Emissions. *ACS Appl. Electron. Mater.* **2021**, *3*, 4144−4150.

(10) Cao, S.; Li, C.; He, P.; Lai, J.; An, K.; Zhou, M.; Feng, P.; Zhou, M.; Tang, X. Ultrahigh Photoluminescence Quantum Yield Organic Manganese Halide Scintillator for X-ray Imaging. *ACS Appl. Opt. Mater.* **2023**, *1*, 623−632.

(11) Zhang, S.; Han, K.; Xia, Z. Pseudohalide Anions Driven Structural Modulation in Distorted Tetrahedral Manganese(II) Hybrids Toward Tunable Green-Red Emissions. *Angew. Chem., Int. Ed.* **2024**, *64*, No. e202419333.
(12) Lun, M.-M.; Ni, H.-F.; Zhang, Z.-X.; Li, J.-Y.; Jia, Q.-Q.; Zhang, Y.; Zhang, Y.; Fu, D.-W. Unusual Thermal Quenching of Photoluminescence from an Organic-Inorganic Hybrid $[MnBr_4]^{2-}$-based Halide Mediated by Crystalline-Crystalline Phase Transition. *Angew. Chem., Int. Ed.* **2024**, *63*, No. e202313590.
(13) Zhang, Y.; Li, Z.-G.; Song, H.; Yang, T.-Y.; Wu, X.; Cai, W.; Zhang, J.; Li, W.; Bu, X.-H. Linear Regulation of Red Emission in an Organic-Inorganic Manganese Bromide via Pressure. *Chem. Mater.* **2024**, *36*, 3435−3443.
(14) She, P.; Ma, Y.; Qin, Y.; Xie, M.; Li, F.; Liu, S.; Huang, W.; Zhao, Q. Dynamic Luminescence Manipulation for Rewritable and Multi-Level Security Printing. *Matter* **2019**, *1*, 1644−1655.
(15) Fu, P.; Sun, Y.; Xia, Z.; Xiao, Z. Photoluminescence Behavior of Zero-Dimensional Manganese Halide Tetrahedra Embedded in Conjugated Organic Matrices. *J. Phys. Chem. Lett.* **2021**, *12*, 7394−7399.
(16) Peng, H.; Huang, T.; Zou, B.; Tian, Y.; Wang, X.; Guo, Y.; Dong, T.; Yu, Z.; Ding, C.; Yang, F.; Wang, J. Organic-Inorganic Hybrid Manganese Bromine Single Crystal with Dual-Band Photoluminescence from Polaronic and Bipolaronic Excitons. *Nano Energy* **2021**, *87*, 106166.
(17) Dai, G.; Ma, Z.; Qiu, Y.; Li, Z.; Fu, X.; Jiang, H.; Ma, Z. A Red-Emitting Hybrid Manganese Halide Perovskite $C_5H_5NOMnCl_2{\cdot}H_2O$ Featuring One-Dimensional Octahedron Chains. *Inorg. Chem.* **2022**, *61*, 12635−12642.
(18) Su, B.; Zhou, G.; Huang, J.; Song, E.; Nag, A.; Xia, Z. Mn^{2+}-Doped Metal Halide Perovskites: Structure, Photoluminescence, and Application. *Laser Photonics Rev.* **2020**, *15*, 2000334.
(19) Song, E.; Jiang, X.; Zhou, Y.; Lin, Z.; Ye, S.; Xia, Z.; Zhang, Q. Heavy Mn^{2+}-Doped $MgAl_2O_4$ Phosphor for High-Efficient Near-Infrared Light-Emitting Diode and the Night-Vision Application. *Adv. Optical Mater.* **2019**, *7*, 1901105.
(20) Song, E.; Ding, S.; Wu, M.; Ye, S.; Xiao, F.; Zhou, S.; Zhang, Q. Anomalous NIR Luminescence in Mn^{2+}-Doped Fluoride Perovskite Nanocrystals. *Adv. Optical Mater.* **2014**, *2*, 670−678.
(21) Bortoluzzi, M.; Castro, J.; Enrichi, F.; Vomiero, A.; Busato, M.; Huang, W. Green-Emitting Manganese(II) Complexes with Phosphoramide and Phenylphosphonic Diamide Ligands. *Inorg. Chem. Commun.* **2018**, *92*, 145.
(22) Huang, X.; Qin, Y.; She, P.; Meng, H.; Liu, S.; Zhao, Q. Functionalized Triphenylphosphine Oxide-Based Manganese(II) Complexes for Luminescent Printing. *Dalton Trans.* **2021**, *50*, 8831.
(23) Bortoluzzi, M.; Ferraro, V.; Castro, J. Synthesis and Photoluminescence of Manganese(II) Naphtylphosphonic Diamide Complexes. *Dalton Trans.* **2021**, *50*, 3132.
(24) She, P.; Zheng, Z.; Qin, Y.; Li, F.; Zheng, X.; Zhang, D.; Xie, Z.; Duan, L.; Wong, W.-Y. Color Tunable Phosphorescent Neutral Manganese(II) Complexes Through Steric Hindrance Driven Bond Angle Distortion. *Adv. Optical Mater.* **2023**, *12*, 2302132.
(25) Tao, P.; Liu, S.-J.; Wong, W.-Y. Phosphorescent Manganese(II) Complexes and Their Emerging Applications. *Adv. Optical Mater.* **2020**, *8*, 2000985.
(26) Chen, J.; Zhang, Q.; Zheng, F.-K.; Liu, Z.-F.; Wang, S.-H.; Wu, A.-Q.; Guo, G.-C. Intense Photo- and Tribo-luminescence of Three Tetrahedral Manganese(II) Dihalides with Chelating Bidentate Phosphine Oxide Ligand. *Dalton Trans.* **2015**, *44*, 3289.
(27) Cotton, F. A.; Goodgame, D. M.; Goodgame, M. Absorption Spectra and Electronic Structures of Some Tetrahedral Manganese-(II) Complexes. *J. Am. Chem. Soc.* **1962**, *84*, 167−172.
(28) Jin, Z.-M.; Tu, B.; Li, Y.-Q.; Li, M.-A. Dichlorobis [phosphonic tris(dimethylamide)] manganese(II). *Acta Crystallogr.* **2005**, *E61*, m2510−m2511.
(29) Zhang, W.; Zheng, W.; Li, L.; Huang, P.; Xu, J.; Zhang, W.; Shao, Z.; Chen, X. Unlocking the Potential of Organic-Inorganic Hybrid Manganese Halides for Advanced Optoelectronic Applications. *Adv. Mater.* **2024**, *36*, 2408777.
(30) Qin, Y.; She, P.; Huang, X.; Huang, W.; Zhao, Q. Luminescent Manganese(II) Complexes: Synthesis, Properties and Optoelectronic Applications. *Coord. Chem. Rev.* **2020**, *416*, 213331.
(31) Hay, M. A.; Sarkar, A.; Marriott, K. E. R.; Wilson, C.; Rajaraman, G.; Murrie, M. Investigation of the Magnetic Anisotropy in a Series of Trigonal Bipyramidal Mn(II) Complexes. *Dalton Trans.* **2019**, *48*, 15480.
(32) Petyuk, M. Y.; Meng, L.; Ma, Z.; Agafontsev, A. M.; Bagryanskaya, I. Y.; Berezin, A. S.; Zhang, J.; Chu, A.; Rakhmanova, M. I.; Meng, H.; Tkachev, A. V.; Yam, V. W.-W.; Artem'ev, A. V. Outstanding Circularly Polarized TADF in Chiral Cu(I) Emitters: From Design to Application in CP-TADF OLEDs. *Angew. Chem., Int. Ed.* **2024**, *63*, No. e202412437.
(33) Lu, J.; Gao, J.; Wang, S.; Xie, M.-J.; Li, B.-Y.; Wang, W.-F.; Mi, J.-R.; Zheng, F.-K.; Guo, G.-C. Improving X-ray Scintillating Merits of Zero-Dimensional Organic-Manganese(II) Halide Hybrids via Enhancing the Ligand Polarizability for High-Resolution Imaging. *Nano Lett.* **2023**, *23*, 4351−4358.
(34) Xu, J.; Luo, R.; Luo, Z.; Xu, J.; Mu, Z.; Bian, H.; Chan, S. Y.; Tan, B. Y. H.; Chi, D.; An, Z.; Xing, G.; Qin, X.; Gong, C.; et al. Ultrabright Molecular Scintillators Enabled by Lanthanide-Assisted Near-Unity Triplet Exciton Recycling. *Nat. Photonics* **2025**, *19*, 71−78.
(35) Mu, D.; Wang, T.; Yuan, J.; Han, L.; Song, H.; Yao, S.; Meng, B.; Wang, T.; Xu, X. X-Ray Real-Time Imaging and Delayed Imaging from Lead-Free Perovskite Scintillators. *Adv. Optical Mater.* **2024**, *12*, 2401455.
(36) Wang, T. C.; Yao, S. Y.; Yan, S. P.; Yu, J.; Deng, Z. Y.; Yakovlev, A. N.; Meng, B.; Qiu, J. B.; Xu, X. H. High Thermal Stability of Copper-Based Perovskite Scintillators for High-Temperature X-ray Detection. *ACS Appl. Mater. Interfaces* **2023**, *15*, 23421−23428.
(37) Li, J.; Hu, Q.; Xiao, J.; Yan, Z. G. High-Stability Double Perovskite Scintillator for Flexible X-ray Imaging. *J. Colloid Interface Sci.* **2024**, *671*, 725−731.

https://doi.org/10.1021/acsaom.5c00040
ACS Appl. Opt. Mater. 2025, 3, 942−948